27/28th International Conference
ENGINEERING MECHANICS 2022
Milovy, Czech Republic, May 9 –12, 2022
Paper **#96,** pp. 329–332, doi: 10.21495/51-2-329

SENSITIVITY STUDY OF A BUBBLE SIZE ON MASS TRANSFER IN A CFD MODEL OF A BUBBLE-COLUMN PHOTOBIOREACTOR

Rebej M.[*], Vondál J.[**], Juřena T.[***], Naď M.[†], Jegla Z.[‡]

Abstract: *The paper deals with the flue gas as a potential nutrient source for microalgae cultivation in photobioreactors. In numerical analyses, the vertical tubular photobioreactor was aerated with an aeration gas modelled through different bubble sizes. This had yielded differences in mass transfer coefficients and interphase areas. The range of bubble diameters extended from -20 % to +20 % from the original bubble diameter 4.50 mm found in the experiment. The assessment of the time to reach the saturated state and the volumetric mass transfer rate did not reveal any discrepancies from analytical predictions. However, even the smallest bubbles did not follow the initial drop of CO_2 volume fraction found in the experiments.*

Keywords: Photobioreactor, Multiphase fluid flow, Mass transfer, CFD, Bubble diameter.

1. Introduction

Cultivation of algae can offer the biotechnological basis for an effective removal of pollutants from waste streams and provide a sustainable way in biomass production at the same time. However, an optimal cultivation technology is a key for the most efficient biomass production. Even though there are algae strains that could tolerate up to 12 % CO_2, the photobioreactor itself can be limiting the overall efficiency (Pulz, 2001). Therefore, it is important to distinguish between the mass-transfer or kinetically limited cultivation system (Kraakman et al., 2011). Often, low gas solubility in the gas-liquid systems is the cause for the mass-transfer limited system (Kraakman et al., 2011). The overall mass transfer rate is dependent on the size of the dispersed phase, i.e. bubble diameter, and the contact time. Both of these parameters can change as the flow is developed through the reactor. The objective of the paper is to study the effect of the bubble size on the mass transfer rate and the time to reach the saturated state.

2. Experimental photobioreactor

Numerical simulations described in this paper followed the design of the pilot experimental bubble column photobioreactor composed of three vertical tubes with the oval cross section. The cultivation medium was aerated from the bottom part of the tubes through the perforated inlet cubes. However, to speed up and reduce the computational load, only one tube limited to 1 m height was modelled.

Aeration gas mixture

The tube was filled with water at an ambient temperature 22 °C. The original composition of the aeration gas that was fed to the reactor from storage is in the Tab. 1. However, to further reduce computational

[*] Ing. Miroslav Rebej: Institute of Process engineering, Brno University of Technology, Technická 2896/2, 616 69, Brno; CZ, rebej@fme.vutbr.cz

[**] Ing. Jiří Vondál, Ph.D.: Institute of Process engineering, Brno University of Technology, Technická 2896/2, 616 69, Brno; CZ, vondal@fme.vutbr.cz

[***] Ing. Tomáš Juřena, Ph.D.: Institute of Process engineering, Brno University of Technology, Technická 2896/2, 616 69, Brno; CZ, jurena@fme.vutbr.cz

[†] Ing. Martin Naď, PhD.: Institute of Process engineering, Brno University of Technology, Technická 2896/2, 616 69, Brno; CZ, nad@fme.vutbr.cz

[‡] doc. Ing. Zdeněk Jegla, Ph.D.: Institute of Process engineering, Brno University of Technology, Technická 2896/2, 616 69, Brno; CZ, jegla@fme.vutbr.cz

demands, aeration gas components with the lowest concentration, i.e. SO_2, CO, and NO, were neglected in numerical simulations.

Tab. 1: Original composition of the aeration gas

Substance	SO_2	CO	NO	O_2	CO_2	N_2
Amount	50 mg m_N^{-3}	50 mg m_N^{-3}	200 mg m_N^{-3}	9 $\%_{vol.}$	10 $\%_{vol.}$	81 $\%_{vol.}$

Under normal operational conditions of the complete pilot photobioreactor, the cultivation medium is aerated with the air flow rate of 2 L/min at 165 mbar. In the experiments, it was observed that the uniform bubbly flow had developed shortly after the air injection with the mean bubble diameter close to 4.5 mm, see Fig. 1.

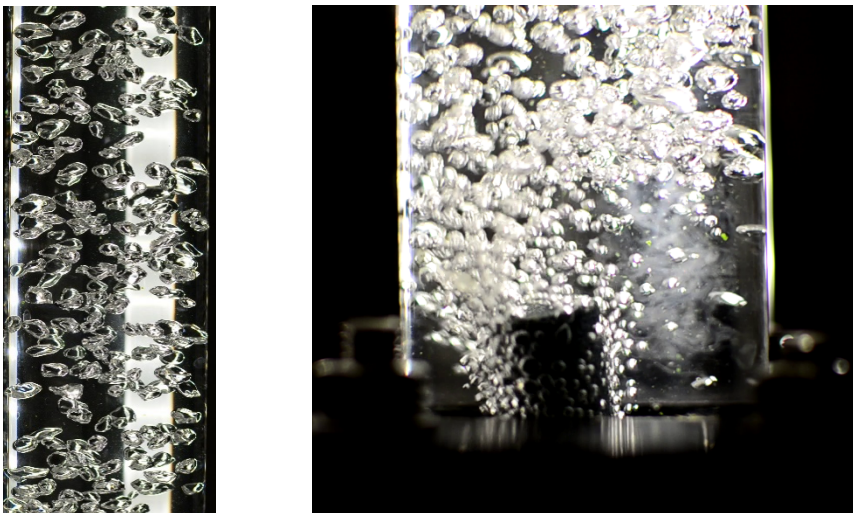

a) b)

Fig. 1: Bubble size and distribution: a) mid-height, b) inlet region.

3. Numerical model

The numerical model is built on a section of one of the three tubes with the height limited to 1 m. The bottom of the domain was placed above the inlet cube where the introduction of air was modelled using the mass-source term. This approach allowed to neglect the geometry of the inlet cube and to distribute the aeration gas uniformly, following observations found in the experiment, see Fig. 1b.

The computational mesh was made in the ANSYS SpaceClaim 2021 R2 (ANSYS Inc., 2021) with 39,288 polyhedral cells with the minimum orthogonal quality of 0.5 and max cell size of 3.77 mm. All but top walls were treated as the no-slip wall for all phases. The top free surface was defined with the degassing boundary condition, i.e. a free-slip wall for the liquid phase and an outlet for the gaseous phase.

The multi-phase numerical model is based on the Eulerian-Eulerian framework found the ANSYS Fluent 2021 R2 (ANSYS Inc., 2021). The primary phase is the liquid water and liquid CO_2, and the secondary phase is the aeration gas with the inlet composition presented in the Chapter 2. The interphase interaction force only included the Ishii-Zuber drag model.

The interphase species mass transfer employed the Henry's law formulation with the molar concentration correlation of 3,030,300 (Pa m3)/kmol (Sander, 2015). Next, to determine the mass transfer coefficient, the penetration model of (Higbie, 1935) was used as it was found to be a suitable mass transfer model for the weakly turbulent flows (Gao et al., 2015), Eq (1).

$$k_L = \sqrt{\frac{4D_L u_{slip}}{\pi d_B}} \tag{1}$$

where the mass-transfer coefficient, k_L, is based on the phase diffusivity, D_L, slip velocity, u_{slip}, and the bubble diameter, d_B. The slip velocity was taken from the numerical simulations of a bubbly flow with neglected mass transfer and was found to be 0.21 m/s. The mass diffusion coefficients for species pairs are listed in Tab.2.

Tab. 2: Diffusion coefficients (Cussler, 2009)

Species pair	$CO_2 - O_2$ (g)	$CO_2 - N_2$ (g)	$N_2 - O_2$ (g)	$H_2O - CO_2$ (l)
Diff. coefficient, cm^2/sec	0.156	0.165	0.220	1.92e-5

Initially, the secondary phase was modelled with the formulation of a spherical bubble with the mean diameter found in experiments, i.e. 4.50 mm, but this was extended to other diameters for the purpose of this paper. Considered mean bubble diameters are ± 10 % and ± 20 % with respect to the original diameter, i.e. 3.60, 4.05, 4.50, 4.95, and 5.40 mm. Tab. 3 shows the volumetric mass transfer coefficient, $k_L a$, as a function of a bubble diameter used in CFD analyses with the interphase area concentration, a, defined according to (2).

$$a = \frac{6}{d_B} \tag{2}$$

Tab. 3: Input for numerical simulation.

d_B	Δd_B	$k_L a$	$\Delta k_L a$
3.60 mm	-20 %	5.004e-6 s^{-1}	+39.75 %
4.05 mm	-10 %	4.194e-6 s^{-1}	+17.12 %
4.50 mm	0 %	3.581e-6 s^{-1}	0 %
4.95 mm	+10 %	3.104e-6 s^{-1}	-13.32 %
5.40 mm	+20 %	2.724e-6 s^{-1}	-23.93 %

Equations for momentum, continuity, volume fraction, energy and interphase species mass transfer were solved with the pressure-based phase-coupled algorithm. The second-order spatial discretization was employed for momentum equations and PRESTO! for the pressure discretization. The numerical model was initialized with the domain filled with quiescent liquid water only.

As the numerical model was reduced to one tube only, the air flow rate in was 0.667 L/min. With mean bubble diameter of 4.5 mm, the respective bubble rising velocity in water can be up to 0.35 m/s. Compared to the mass-transfer coefficient, it can be concluded that the time-scale is defined by the hydrodynamic phenomenon. So, considering 4 mm cell size, the time step size 0.005 s yields the Courant number of 0.5.

4. Results and conclusions

The Fig. 2 shows the results of a CO_2 volume fraction obtained from CFD analyses and experiment. In the experiment, the measurement probe was positioned at the tube outlet. Similarly, the CO_2 volume fraction was monitored at the domain's top surface in CFD analyses. On the other hand, Fig. 3. shows the average mass transfer rate of CO_2 from the gaseous phase to the liquid phase.

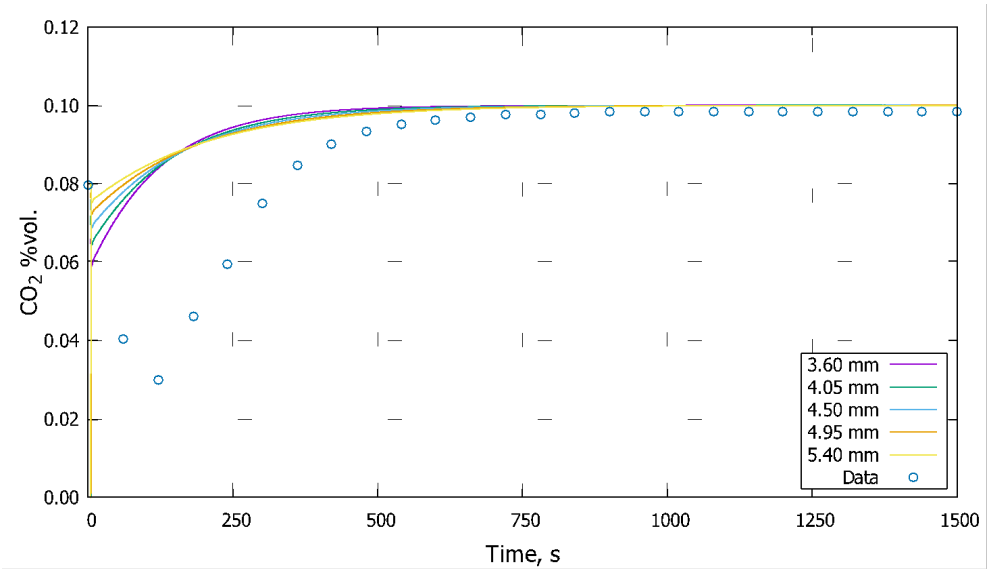

Fig. 2: CO_2 volume fraction, CFD analyses and experimental data

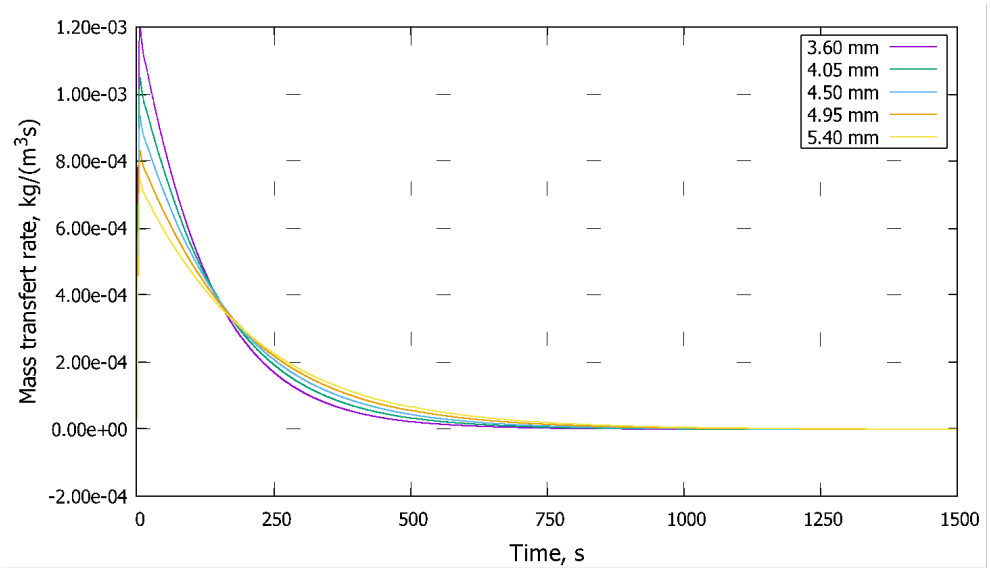

Fig. 3: Mass transfer rate

Mass transfer rate is predicted within the expected range, i.e. up to +39.5 % increase for the 3.60 mm bubbles and up to -24.0 % decrease for the 5.40 mm bubbles. These differences are observable for the first 3 minutes. Later, the concentration gradient dominates the overall mass transfer rendering the bubble size insignificant. In all cases, the liquid is saturated after approximately 12.5 minutes (750 s).

The results proved that as the bubbles get smaller, they offer larger interfacial area and the mass transfer rate is enhanced. Consequently, reducing the amount of CO_2 in the gaseous phase. However, no analysis predicted such significant drop of the CO_2 volume fraction as it was found in the experiment. The reason might be a combination of the fact that the bubbles leaving the inlet are even smaller in size and, therefore, offer even larger interfacial area, and the fact that the concentration gradient at the beginning is the largest. Therefore, more detailed analysis with wider range of bubble sizes and the inclusion of the inlet cube could potentially yield more accurate results. Also, implementation of a different mass-transfer coefficient model could be beneficial, there.

Acknowledgement

This research was supported by the EU project Strategic Partnership for Environmental Technologies and Energy Production, funded as project No. CZ.02.1.01/0.0/0.0/16_026/0008413 by Czech Republic Operational Programme Research, Development and Education, Priority Axis 1: Strengthening capacity for high-quality research.

Miroslav Rebej is the Brno Ph.D. Talent Scholarship Holder – Funded by the Brno City Municipality.

References

ANSYS Inc., (2021). *ANSYS Fluent Theory Guide, Release 2021 R2.* ANSYS Inc., Canonsburg, PA, USA.

Cussler, E.L., (2009). *Diffusion: Mass Transfer in Fluid Systems*, Cambridge Series in Chemical Engineering. Cambridge University Press.

Gao, X., Kong, B., Ramezani, M., Olsen, M.G., and Vigil, R.D., (2015). An adaptive model for gas-liquid mass transfer in a Taylor vortex reactor. *International Journal of Heat and Mass Transfer* 91, 433–445. https://doi.org/10.1016/j.ijheatmasstransfer.2015.07.125

Higbie, R., (1935). The rate of absorption of a pure gas into still liquid during short periods of exposure. *Transactions of the American Institute of Chemical Engineers* 31, 365–377.

Kraakman, N.J.R., Rocha-Rios, J., and van Loosdrecht, M.C.M., (2011). Review of mass transfer aspects for biological gas treatment. *Applied Microbiology and Biotechnology* 91, 873–886. https://doi.org/10.1007/ s00253-011-3365-5

Pulz, O., 2001. Photobioreactors: production systems for phototrophic microorganisms. *Applied Microbiology and Biotechnology* 57, 287–293. https://doi.org/10.1007/s002530100702

Sander, R., 2015. Compilation of Henry's law constants (version 4.0) for water as solvent. *Atmospheric Chemistry & Physics* 15, 4399–4981. https://doi.org/10.5194/acp-15-4399-2015